Extended Data Figure 1

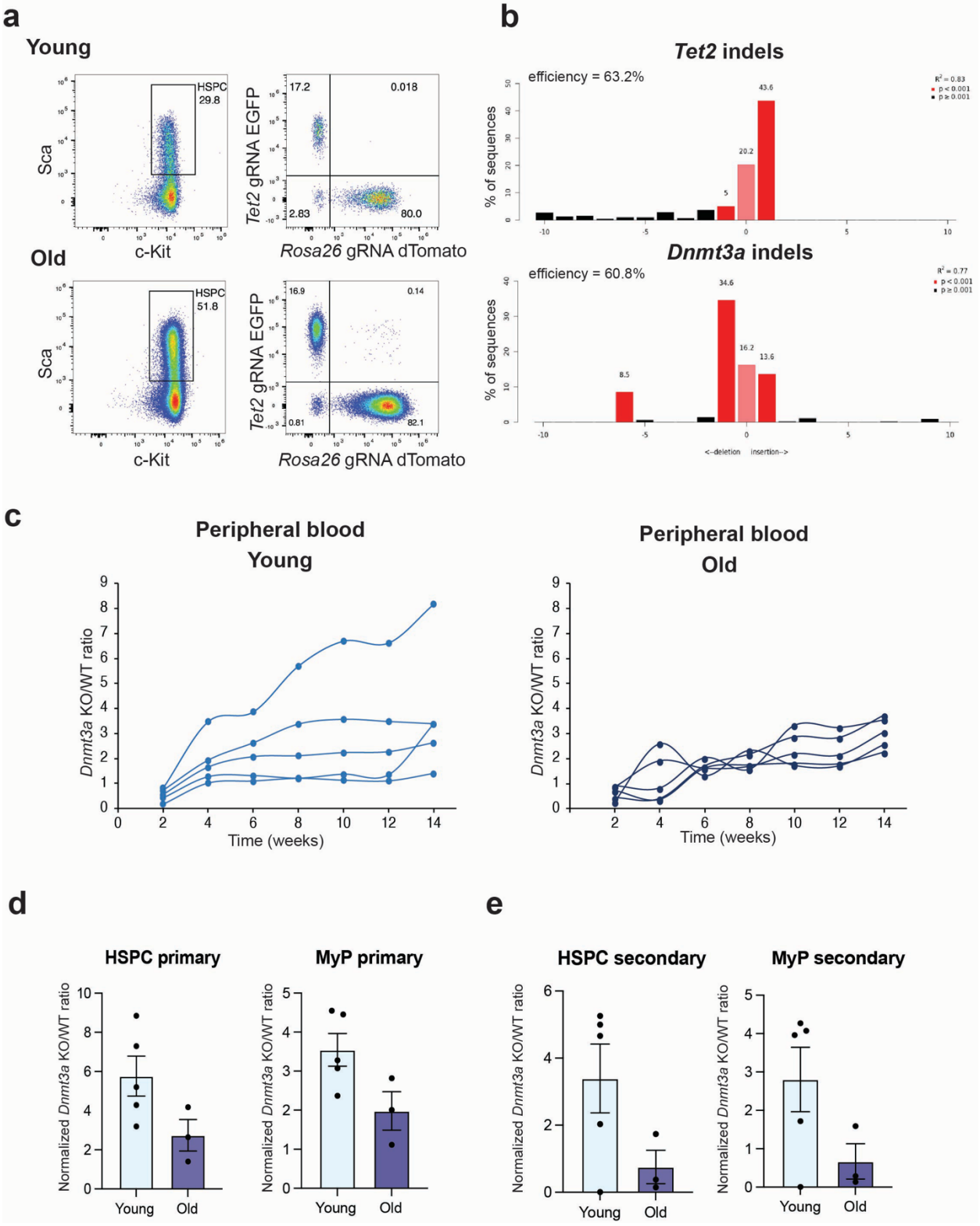

Extended Data Fig. 1 | *Dnmt3a* KO hematopoietic cells are not selected with aging. **a**) representative flow cytometry analysis of donor cells at the end of the in vitro CRISPR protocol, at the time of transplantation; left panels are gated on live, lineage^{NEG} cells, right panels are gated on HSPC. **b**) results from TIDE analysis of PCR products spanning the genomic target regions of *Tet2* CRISPR (top) or *Dnmt3a* CRISPR (bottom) from cells subjected to CRISPR for the indicated genes. **c**) Ratio of *Dnmt3a* KO/WT cells over time in the peripheral blood of recipient young or old mice. **d-e**) relative *Dnmt3a* KO/WT expansion normalized by the ratio of transplanted cells in the bone marrow MyP or HSC of recipient mice at 16 weeks after primary transplantation (**d**) or 16 weeks after secondary transplantation (**e**).

Extended Data Figure 2

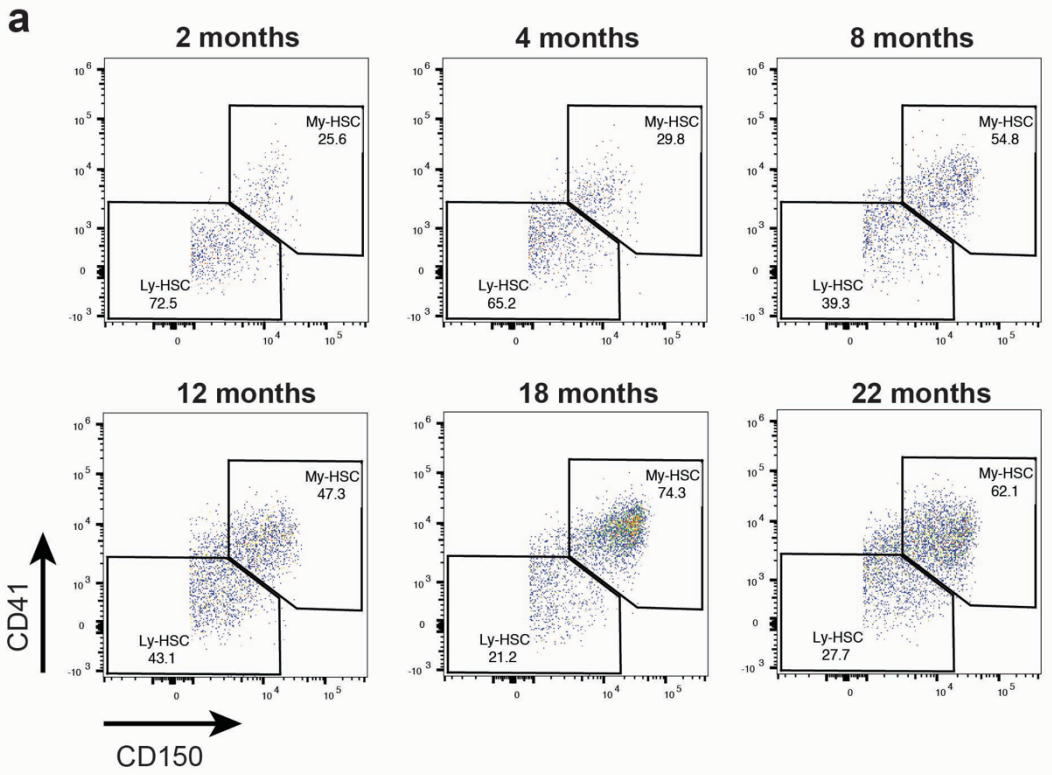

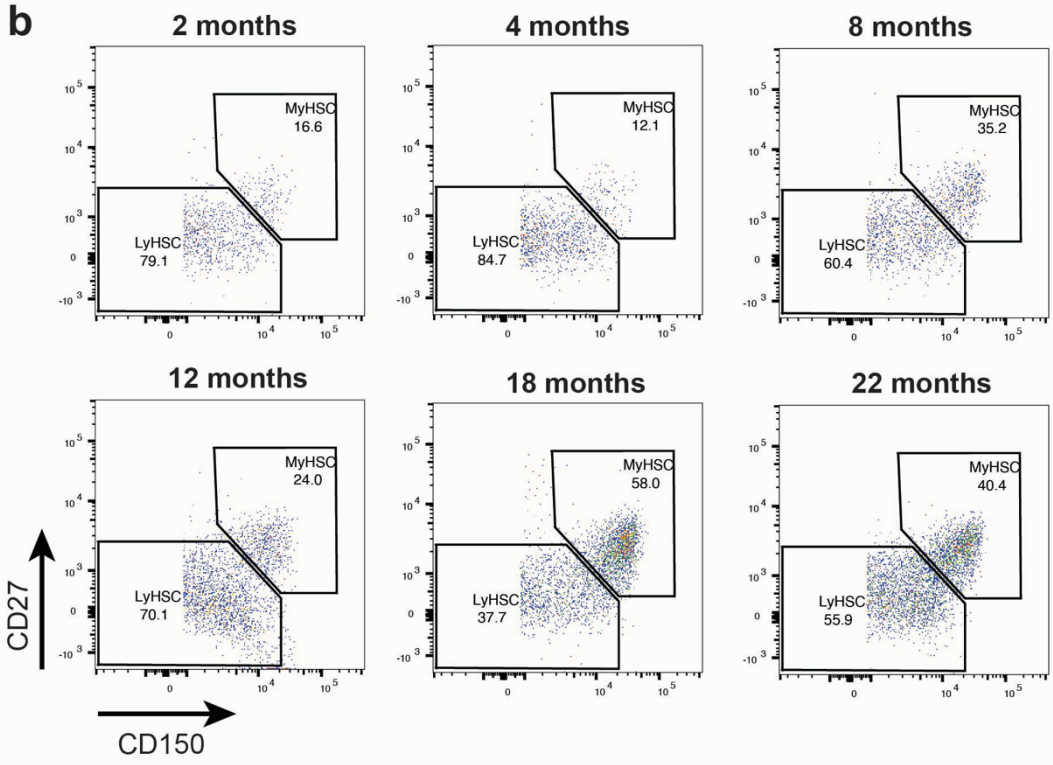

Extended Data Fig. 2 | Aging is associated with increased flow cytometry detection of myeloid biased HSC expressing CD150, CD41 and CD27. Flow cytometry analysis of bone marrow HSC from female mice of the indicated ages and MyHSC quantification by CD150-CD41 expression (**a**) or CD150-CD27 expression (**b**).

Extended data Figure 3

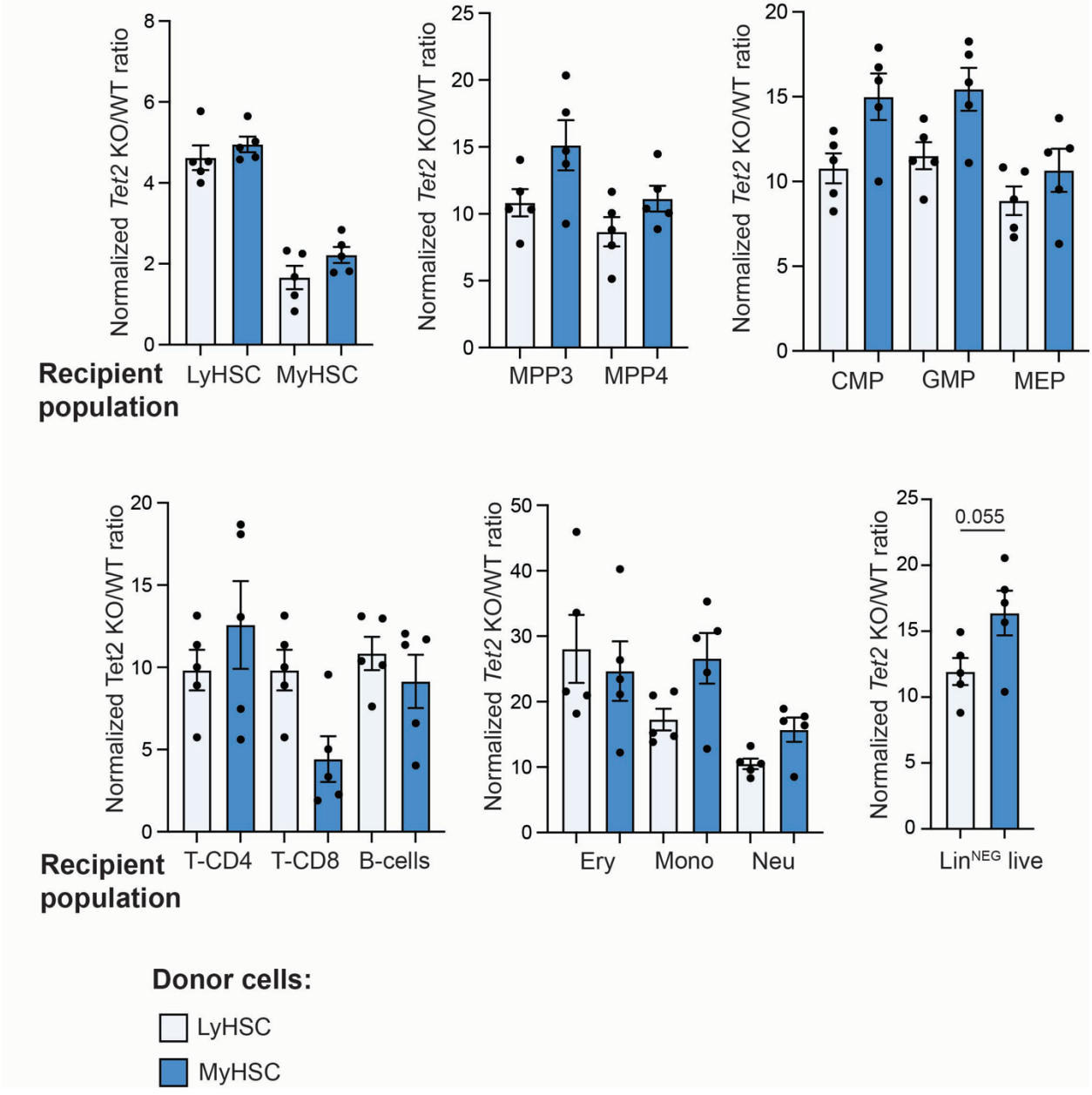

Extended Data Fig. 3 | *Tet2* KO cells from aged donor MyHSC or LyHSC show similar levels of selection. Relative *Tet2* KO/WT expansion normalized by the ratio of transplanted cells for the indicated donor LyHSC of MyHSC cells in the different populations in the bone marrow of recipient mice 12 weeks post-transplantation.

Extended Data Figure 4

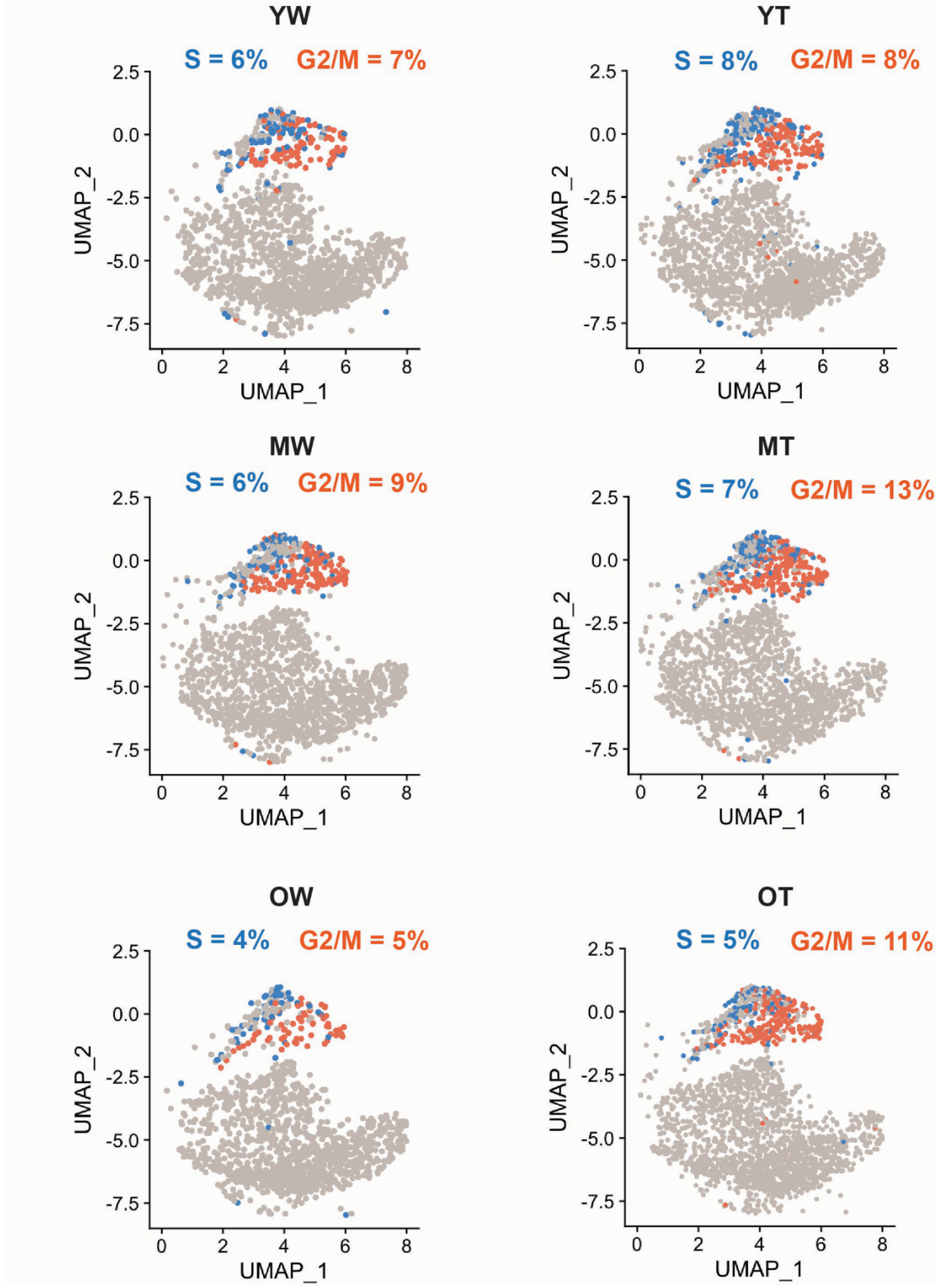

Extended data Fig. 4 | Reduced cycling HSC with aging are rescued by *Tet2* KO. Colored UMAP for cell cycle analysis displaying S and G/2M fraction of cells in LT + ST-HSC based on gene expression.

Extended Data Figure 5

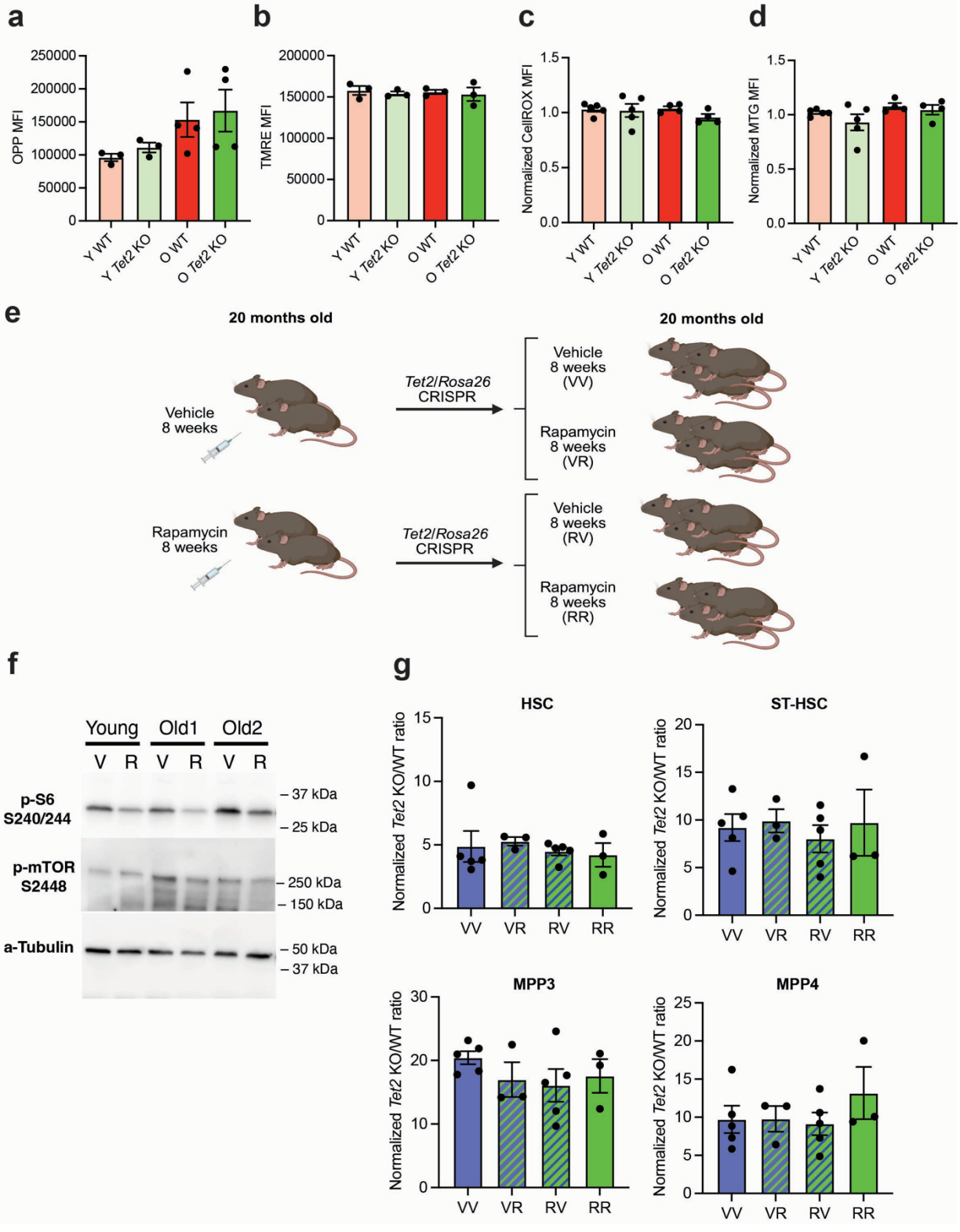

Extended Data Fig. 5 | Selection of *Tet2* KO cells with aging is not dependent on alterations in mitochondrial and ribosomal functions. **a**) Analysis of translation efficiency by OPP staining of the indicated populations in the bone marrow 12 weeks post competitive transplantation of *Tet2* KO or WT cells. **b**) Analysis of mitochondrial membrane potential by TMRE staining of the indicated populations in the bone marrow 12 weeks post non-competitive transplantation of *Tet2* KO or WT cells (EGFP tagged transplanted in different mice). **c-d**) analysis of ROS abundance by CellROX staining (**c**) or mitochondrial mass by MTG staining (**d**) of the indicated populations in the bone marrow 12 weeks post non-competitive transplantation of *Tet2* KO or WT cells (dTomato tagged transplanted in different mice). **e**) Experimental design of rapamycin intervention to assess the role in *Tet2* KO age-related expansion. **f**) Immunoblot analysis of c-Kit-enriched bone marrow cells from one young or two old non-transplanted mice administered one dose of rapamycin and sacrificed 12 hours later. **g**) Relative *Tet2* KO/WT expansion in the indicated recipient BM populations normalized by the ratio of transplanted cells from mice treated with rapamycin or vehicle as indicated.

Supplementary Table 1. Ribosomal protein genes modulating p53.

Ribosomal protein	References
RPL11	Zhang et al. Molecular Cell Biology 2003[1]
RPL15	Shi et al. Cancer Cell International 2022[2]
RPL22	Cao et al. Oncotarget 2017[3]; Jansen et al. Cell Reports 2024[4]
RPL23	Dai et al. Molecular Cell Biology 2004[5]
RPL26	Ofir-Rosenfeld et al. Molecular Cell 2008[6]
RPL37	Llanos et al. Cell Cycle 2010[7], Daftuar et al. PLOS 2013[8]
RPL4	He et al. Oncotarget 2015[9]
RPL5	Dai et al. Journal of Biol Chem 2004[10]
RPL6	Bai et al. Nuclei Acid Research 2014[11]
RPS14	Zhou et al. Oncogene 2013[12]
RPS15	Daftuar et al. PLOS 2013[8]
RPS15A	Chen et al. Inern Journal of Oncology 2016[13]
RPS2	Cho et al. Biochem and Bioph Res Comm 2020[14]
RPS20	Daftuar et al. PLOS 2013[8]
RPS25	Zhang et al. Oncogene 2013[15]
RPS26	Cui et al Oncogene 2014[16]
RPS27	Xiong et al. Oncogene 2011[17]
RPS27A	Sun et al. Journ of Biolog Chem 2011[18]
RPS27L	Xiong et al. Oncogene 2011[17]
RPS3	Yadavilli et al. DNA repair 2009[19]
RPS7	Sun et al. Journ of Biolog Chem 2011[18]

Supplementary Methods

Flow cytometry

All flow cytometry experiments were analyzed with a BD CytoFLEX flow cytometer equipped with violet, blue, yellow and red lasers.

Peripheral blood was stained with the following antibody panel: Per-CP Cyanine 5.5. anti mouse GR1 1:200, PE-Cyanine7 anti-mouse CD11b 1:200, APC-Cyanine 7 anti-mouse CD4 1:200, APC-Cyanine 7 anti-mouse CD8a 1:200, BV785 anti-mouse CD45R/B220 1:200, TruStain FcX (anti-mouse CD16/32) 1:100. Blood cell populations were defined as follows: Neutrophils ($DAPI^{NEG}$, $CD11b^{+}$, $GR1^{+}$), Monocytes ($DAPI^{NEG}$, $CD11b^{+}$, $GR1^{NEG}$), B-cells ($DAPI^{NEG}$, $B220^{+}$), T-cells ($DAPI^{NEG}$, $CD4^{+}$/$CD8a^{+}$).

Bone marrow “Mature” antibody panel was as follows: APC anti-mouse c-Kit 1:100, PE-Cyanine7 anti-mouse CD11b 1:200, Brilliant Violet 605 anti mouse CD45R/B220 1:100, Pacific Blue anti-mouse TER-119 1:200, Per-CP Cyanine 5.5 anti-mouse GR1 1:200, Alexa Fluor anti-mouse CD8a 1:200, Brilliant Violet 510 anti-mouse CD4 1:200, Brilliant Violet 785 anti-mouse Ly6C 1:200, Near-IR Dead Cell Stain Kit 1:200, TruStain FcX (anti-mouse CD16/32) 1:100. Cells were stained in 50 µL of FACS buffer for 30 minutes, at 4 ºC, in the dark. Cell populations were defined as follows: neutrophils ($Near\text{-}IR^{NEG}$, $c\text{-}Kit^{NEG}$, $CD11b^{+}$, $Ly\text{-}6C^{low}$, $GR1^{+}$), monocytes ($Near\text{-}IR^{-}$, $c\text{-}Kit^{NEG}$, $CD11b^{+}$, $Ly\text{-}6C^{+}$, $GR1^{low}$), B-cells ($Near\text{-}IR^{NEG}$, $c\text{-}Kit^{NEG}$, $B220^{+}$), erythroid cells ($Near\text{-}IR^{NEG}$, $c\text{-}Kit^{-}$, $TER\text{-}119^{+}$), $CD4^{+}$ T-cells ($Near\text{-}IR^{NEG}$, $c\text{-}Kit^{NEG}$, $CD8a^{-}$, $CD4^{+}$), $CD8^{+}$ T-cells ($Near\text{-}IR^{NEG}$, $c\text{-}Kit^{NEG}$, $CD4^{NEG}$, $CD8a^{+}$).

Bone Marrow “Progenitor” antibody panel was as follows: lineage cocktail (APC-Cyanine 7 anti-mouse TER-119 1:100, APC-Cyanine 7 anti-mouse CD3e 1:100, APC-Cyanine 7 anti-mouse CD8a 1:200, APC-Cyanine 7 anti-mouse CD45R/B220 1:200, APC-Cyanine 7 anti-mouse CD11b 1:200, APC-Cyanine 7 anti-mouse GR1 1:200), Brilliant Violet 785 anti-mouse Sca 1:100, PE-Cyanine 7 anti-mouse c-Kit 1:100, eFluor 660 anti-mouse CD34 1:200, APC-R700 anti-mouse CD16/32 1:100, Brilliant Violet 421 anti-mouse CD135 1:100, Brilliant Violet 711 anti-mouse CD127 1:100, Near-IR Dead Cell Stain Kit

1:200, IgG from rat serum 50 µg/mL. Cells were stained in 50 µL of FACS buffer for 30 minutes, at 4 ºC, in the dark. Cell populations were defined as follows: myeloid progenitors/MyP (Near-IR^{NEG}, lineage^{NEG}, c-Kit^{+}, Sca^{NEG}), common lymphoid progenitors/CLP (Near-IR^{NEG}, lineage^{NEG}, c-Kit^{low}, Sca^{low}, CD127^{+}, CD135^{+}) common myeloid progenitors/CMP (Near-IR^{NEG}, lineage^{NEG}, c-Kit^{+}, Sca^{NEG}, CD34^{+}, CD16/32^{NEG}), granulocyte-monocyte progenitors (Near-IR^{NEG}, lineage^{NEG}, c-Kit^{+}, Sca^{NEG}, CD34^{+}, CD16/32^{+}), megakaryocyte erythrocyte progenitors/MEP (Near-IR^{NEG}, lineage^{NEG}, c-Kit^{+}, Sca^{NEG}, CD34^{NEG}, CD16/32^{NEG}).

Bone Marrow “Stem” antibody panel was as follows: lineage cocktail (see above), APC-Anti mouse Sca 1:100, PE-Cyanine 7 anti-mouse c-Kit 1:100, Brilliant Violet 421 anti-mouse CD135, Alexa Fluor 700 anti-mouse CD48 1:100, Brilliant Violet 785 anti-mouse CD150 1:100, Brilliant Violet 711 anti-mouse CD41 1:100, IgG from rat serum 50 µg/mL. Cells were stained in 100 µL of FACS buffer for 30 minutes, at 4 ºC, in the dark. Cell population were defined as follows: myeloid progenitors/MP (Near-IR^{NEG}, lineage^{-}, c-Kit^{+}, Sca^{NEG}), HSPC (Near-IR^{NEG}, lineage^{NEG}, c-Kit^{+}, Sca^{+}), MPP4 (Near-IR^{NEG}, lineage^{NEG}, c-Kit^{+}, Sca^{+}, CD135^{+}), MPP3 (Near-IR^{NEG}, lineage^{-}, c-Kit^{+}, Sca^{+}, CD135^{NEG}, CD48^{+}, CD150^{NEG}), MPP2 (Near-IR^{NEG}, lineage^{NEG}, c-Kit^{+}, Sca^{+}, CD135^{NEG}, CD48^{+}, CD150^{+}), short-term HSC/ST-HSC (Near-IR^{NEG}, lineage^{NEG}, c-Kit^{+}, Sca^{+}, CD135^{NEG}, CD48^{NEG}, CD150^{NEG}), HSC (Near-IR^{NEG}, lineage^{NEG}, c-Kit^{+}, Sca^{+}, CD135^{NEG}, CD48^{NEG}, CD150^{+}), lymphoid-biased HSC/LyHSC (Near-IR^{NEG}, lineage^{NEG}, c-Kit^{+}, Sca^{+}, CD135^{NEG}, CD48^{NEG}, CD150^{low}, CD41^{NEG}), myeloid biased HSC/MyHSC (Near-IR^{NEG}, lineage^{NEG}, c-Kit^{+}, Sca^{+}, CD135^{NEG}, CD48^{NEG}, CD150^{high}, CD41^{+}).

For RNA FISH-Flow cells were stained with the following antibody cocktail: APC-Cyanine 7 anti-mouse TER-119 1:100, APC-Cyanine 7 anti-mouse CD3e 1:100, APC-Cyanine 7 anti-mouse CD8a 1:200, APC-Cyanine 7 anti-mouse CD45R/B220 1:200, APC-Cyanine 7 anti-mouse CD11b 1:200, APC-Cyanine 7 anti-mouse GR1 1:200 Brilliant Violet 785 anti-mouse Sca 1:100, Brilliant Violet 711 anti-mouse c-Kit 1:100, Alexa Fluor 700 anti mouse CD48 1:100, Brilliant Violet 605 anti mouse CD150 1:100, IgG from rat serum 50 µg/mL.

For OPP analysis cells were stained with the following antibody cocktail: lineage cocktail (APC-Cyanine 7 anti-mouse TER-119 1:100, APC-Cyanine 7 anti-mouse CD3e 1:100, APC-Cyanine 7 anti-mouse CD8a 1:200, APC-Cyanine 7 anti-mouse CD45R/B220 1:200, APC-Cyanine 7 anti-mouse CD11b 1:200, APC-Cyanine 7 anti-mouse GR1 1:200), Brilliant Violet 421 anti-mouse Sca 1:100, PE-Cyanine 7 anti-mouse c-Kit 1:100, Brilliant Violet 785 anti-mouse CD150 1:100, Alexa Fluor 700 anti mouse CD48 1:100, IgG from rat serum 50 µg/mL.

For TMRE assay cells were stained with the following antibody cocktail: lineage cocktail (APC-Cyanine 7 anti-mouse TER-119 1:100, APC-Cyanine 7 anti-mouse CD3e 1:100, APC-Cyanine 7 anti-mouse CD8a 1:200, APC-Cyanine 7 anti-mouse CD45R/B220 1:200, APC-Cyanine 7 anti-mouse CD11b 1:200, APC-Cyanine 7 anti-mouse GR1 1:200), APC anti-mouse Sca 1:100, PE-Cyanine 7 anti-mouse c-Kit 1:100, Brilliant Violet 785 anti-mouse CD150 1:100, Brilliant Violet 421 anti mouse CD135 1:100, Alexa Fluor 700 anti mouse CD48 1:100, Near-IR Dead Cell Stain Kit 1:200, IgG from rat serum 50 µg/mL.

For MTG and CellROX assay cells were stained with the following antibody cocktail: (APC-Cyanine 7 anti-mouse TER-119 1:100, APC-Cyanine 7 anti-mouse CD3e 1:100, APC-Cyanine 7 anti-mouse CD8a 1:200, APC-Cyanine 7 anti-mouse CD45R/B220 1:200, APC-Cyanine 7 anti-mouse CD11b 1:200, APC-Cyanine 7 anti-mouse GR1 1:200), APC anti-mouse Sca 1:100, Brilliant violet 711 anti-mouse c-Kit 1:100, Brilliant Violet 785 anti-mouse CD150 1:100, Brilliant Violet 421 anti mouse CD135 1:100, Alexa Fluor 700 anti mouse CD48 1:100, IgG from rat serum 50 µg/mL.

Supplementary table 2. Reagents and resources details.

REAGENT or RESOURCE	SOURCE	IDENTIFIER
Antibodies		
APC-Cyanine 7 anti-mouse TER-119	Biolegend	Cat#116223
APC-Cyanine 7 anti-mouse CD3e	Biolegend	Cat#100330
APC-Cyanine 7 anti-mouse CD4	Biolegend	Cat#100526
APC-Cyanine 7 anti-mouse CD8a	Biolegend	Cat#100714
APC-Cyanine 7 anti-mouse CD45RB220	Biolegend	Cat#103224
APC-Cyanine 7 anti-mouse Ly-6G/Ly-6C (GR-1)	Biolegend	Cat#108424
APC Cyanine 7 anti-moue CD11b	BD	Cat#557657
APC anti-moue Ly-6A/E (Sca-1)	eBioscience	Cat#17-5981-83
PE-Cyanine 7 anti-mouse CD117 (c-Kit)	eBioscience	Cat#25-1171-82
PE-Cyanine 7 anti-mouse CD11b	eBioscience	Cat#25-0112-82
FITC anti mouse CD48	Biolegend	Cat#103404
Alexa Fluor 700 anti mouse CD48	Biolegend	Cat#103426
Brilliant Violet 421 anti-mouse CD150	Biolegend	Cat#115943
Brilliant Violet 605 anti-mouse CD150	Biolegend	Cat#115937
Brilliant Violet 785 anti-mouse CD150	Biolegend	Cat#115927
Brilliant Violet 711 anti-mouse CD127	Biolegend	Cat#135035
Brilliant Violet 421 anti-mouse CD135	Biolegend	Cat#135314
Brilliant Violet 711 anti-mouse CD41	BD	Cat#740712
Brilliant Violet 785 anti-mouse CD45R/B220	Biolegend	Cat#103246
Brilliant Violet 605 anti-mouse CD45R/B220	Biolegend	Cat#103244
Brilliant Violet 510 anti mouse CD4	Biolegend	Cat#100559
Brilliant Violet 785 anti-mouse Ly-6C	Biolegend	Cat#128041
Brilliant Violet 711 anti-mouse CD117 (c-Kit)	Biolegend	Cat#105835
PE/Dazzle 594 anti-mouse CD41	Biolegend	Cat#133935
PE/Dazzle 594 anti-mouse IL27Ra	Biolegend	Cat#159007
eFluor 660 anti-mouse CD34	eBioscience	Cat#50-0341-82
APC-R700 anti-mouse CD16/CD32	BD	Cat#565502
Alexa Fluor 700 anti-mouse CD8a	Biolegend	Cat#100730
Pacific Blue anti-mouse TER-119	Biolegend	Cat#116208
PE-Cyanine 7 anti-mouse CD11b	eBioscience	Cat#25-0112-82
PE anti-mouse TER-119	Biolegend	Cat#116223
PE anti-mouse CD3e	BD	Cat#553064
PE anti-mouse CD4	Biolegend	Cat#100408
PE anti-mouse CD8a	Biolegend	Cat#162304
PE anti-mouse CD45RB220	BD	Cat#553090
PE anti-mouse Ly-6G/Ly-6C (GR-1)	eBioscience	Cat#12-5931-82
PE anti-mouse CD11b	BD	Cat#557397
PerCP Cyanine 5.5 anti-mouse Ly-6G/Ly-6C (GR-1)	Biolegend	Cat#108428
APC anti-mouse CD201 (EPCR)	Biolegend	Cat#141506
APC anti mouse CD117 (c-Kit)	BD	Cat#555356
TruStain FcX (anti-mouse CD16/32)	Biolegend	Cat#101320
Anti-Mouse CD4 [Clone GK1.5]	Leinoco	Cat#C1333
Anti-Mouse CD8a (Ly 2.2) [Clone 2.43]	Leinoco	Cat#C380

CD117 MicroBeads, mouse	Miltenyi	Cat#130-097-146
IgG from rat serum	Millipore Sigma	Cat#I4131-50MG
Phospho-S6 Ribosomal Protein (Ser240/244)	CST	Cat#2215S
Phospho-mTOR (Ser2448)	CST	Cat#2971S
Anti-TUBA4A (TUBA1) Antibody	Millipore Sigma	Cat#T6199
Goat Anti-Rabbit IgG (H + L)-HRP Conjugate	Biorad	Cat#1706515
Goat Anti-Mouse IgG (H + L)-HRP Conjugate	Biorad	Cat#1706516
Chemicals, peptides, and recombinant proteins		
PEI MAX® - Transfection Grade Linear Polyethylenimine Hydrochloride (MW 40,000)	Polysciences	Cat#25765
Poly(vinyl alcohol) average Mw 146,000-186,000, 87-89% hydrolyzed	Millipore Sigma	Cat#363103
Human Fibronectin	Millipore Sigma	Cat#FC010
SCF, Mouse	Genescript	Cat#Z02997-10
TPO, Mouse	Genescript	Cat#Z03175-50
Insulin-Transferrin-Selenium-Ethanolamine (ITS -X) (100X)	Gibco	Cat#51500056
DMEN, high glucose, pyruvate	Gibco	Cat#11995065
IMDM	Gibco	Cat#12440053
Ham's F12 Nutrient Mix	Gibco	Cat#11765054
Penicillin-Streptomycin (10,000 U/mL)	Gibco	Cat#15140122
HEPES (1M)	Gibco	Cat#15630080
Fisherbrand™ Research Grade Fetal Bovine Serum, Canadian Sourced	Fischer Scientific	Cat#FB12999102
Sucrose	Millipore Sigma	Cat#S0389-5KG
Histopaque®-1119	Millipore Sigma	Cat#11191-6X100ML
DAPI	ThermoFisher	Cat#D3571
Ammonium Chloride	Fischer Scientific	Cat#A661-500
Potassium bicarbonate	Millipore Sigma	Cat#237205-500G
O-propargyl puromycin	Vector Labs	Cat#CCT-1407-25
Rapamycin	MedChemExpress	Cat#AY-22989
Tetramethylrhodamine, Ethyl Ester, Perchlorate (TMRE)	ThermoFisher	Cat#T669
CellROX™ Green Reagent, for oxidative stress detection	ThermoFisher	Cat#C10444
MitoTracker™ Green FM Dye, for flow cytometry	ThermoFisher	Cat#M46750
Sodium dodecyl sulphate	Millipore Sigma	Cat#L5750
Tween-20	ThermoFisher	Cat#BP330-500
Tris Base	ThermoFisher	Cat#BP152-5
Bromophenol Blue	Fisher Scientific	Cat# AC403151000
Sodium chloride	Fisher Scientific	Cat#S-6713
Immobilon Western Chemiluminescent HRP Substrate	Millipore Sigma	Cat# WBKLS0500
Glycerol	Fisher Scientific	Cat#BP229-1
Critical commercial assays		
T7-FlashScribe™ Transcription Kit	Cellscript	Cat#C-ASF3507
ScriptCap™ Cap 1 Capping System	Cellscript	Cat#C-SCCS1710

RNeasy Plus Micro Kit	Qiagen	Cat#74034
DNeasy Blood and Tissue Kit	Qiagen	Cat#69506
Plasmid Plus Maxi Kit	Qiagen	Cat#12943
LIVE/DEAD™ Fixable Near-IR Dead Cell Stain Kit, for 633 or 635 nm excitation	ThermoFisher	Cat#L10119
UltraComp eBeads™ Compensation Beads	ThermoFisher	Cat#01-2222-42
LS columns	Miltenyi	Cat#130-042-401
Click-&-Go® Plus 647 OPP	Vector labs	Cat#CTT-1496
BD Cytofix/Cytoperm™ Fixation/Permeabilization Kit	BD	Cat#554714
4-20% acrylamide mini protean TGX precast gels	Biorad	Cat#4561095
Phusion™ High-Fidelity DNA Polymerase	NEB	Cat#M0530L
Deposited data		
Aging and *Tet2* KO mouse scRNAseq data	GEO	GSE310533
Experimental models: Cell lines		
HEK293T cells	Takara	Cat#632180
Experimental models: Organisms/strains		
C57BL6/J	Jackson laboratories	Cat#000664
C57BL/6JN	National Institute on Aging	https://www.nia.nih.gov/research/dab/aged-rodent-colonies
Oligonucleotides		
Mouse *Tet2* gRNA: GGTATATCGGAGATCGAGTG	IDT (design: this paper)	N/A
Mouse *Rosa26* gRNA: GCAATACCATGCCAGGTGGA	IDT (design: this paper)	N/A
Mouse *Dnmt3a* gRNA: CAGGCCGAATTGTGTCTTGG	IDT (design: this paper)	N/A
Mouse *Tet2* FW TIDE: ATTCAAGCCCCTCTGGAGAA	IDT (design: this paper)	N/A
Mouse *Tet2* REV TIDE: CCCACTCTATAGCTGGGCAAT	IDT (design: this paper)	N/A
Mouse *Rosa26* FW TIDE: CCACATTGGCACCATAGTCA	IDT (design: this paper)	N/A
Mouse *Rosa26* REV TIDE: AGCCATCTGGGCCTTTTAAC	IDT (design: this paper)	N/A
Mouse *Dnmt3a* FW TIDE: GCTTGGCTTTGTCACCTGAT	IDT (design: this paper)	N/A
Mouse *Dnmt3a* REV TIDE: CAGCTCAGTGATGGTGGCTA	IDT (design: this paper)	N/A
Recombinant DNA		
pLCv2_U6.(BsmBI).chRNA2_EFS.EGFP_wPRE	Yudovich et al.	N/A
pLCv2_U6.(BsmBI).chRNA2_EFS.dTomato_wPRE	Yudovich et al. (dTomato inserted)	N/A
pMD2.G	Addgene	Cat#12259
psPAX2	Addgene	Cat#12260
pCas9-polyA	Addgene	Cat#79602
Software and algorithms		
FlowJo™ v11	BD	https://flowjo.com/flowjo/overview
GraphPad Prism v10	Dotmatics	https://www.graphpad.com/features
Biorender	Biorender	https://www.biorender.com

Shinyapps	Anschutz Bioinformatic Core	https://bioinformatics.cuanschutz.edu
CRISPick	CRISPick	https://portals.broadinstitute.org/gppx/crispick/public
Illustrator	Adobe	https://www.adobe.com/creativecloud/plans.html?plan=edu&product=illustrator
Primer3	Primer3	http://frodo.wi.mit.edu/primer3/
Heatmapper	Heatmapper	http://heatmapper.ca

Supplementary references

1. Zhang, Y., Wolf, G.W., Bhat, K., Jin, A., Allio, T., Burkhart, W.A., and Xiong, Y. (2003). Ribosomal protein L11 negatively regulates oncoprotein MDM2 and mediates a p53-dependent ribosomal-stress checkpoint pathway. Mol Cell Biol *23*, 8902-8912. 10.1128/mcb.23.23.8902-8912.2003.

2. Shi, R., and Liu, Z. (2022). RPL15 promotes hepatocellular carcinoma progression via regulation of RPs-MDM2-p53 signaling pathway. Cancer Cell Int *22*, 150. 10.1186/s12935-022-02555-5.

3. Cao, B., Fang, Z., Liao, P., Zhou, X., Xiong, J., Zeng, S., and Lu, H. (2017). Cancer-mutated ribosome protein L22 (RPL22/eL22) suppresses cancer cell survival by blocking p53-MDM2 circuit. Oncotarget *8*, 90651-90661. 10.18632/oncotarget.21544.

4. Jansen, J., Bohnsack, K.E., Böhlken-Fascher, S., Bohnsack, M.T., and Dobbelstein, M. (2024). The ribosomal protein L22 binds the MDM4 pre-mRNA and promotes exon skipping to activate p53 upon nucleolar stress. Cell Rep *43*, 114610. 10.1016/j.celrep.2024.114610.

5. Dai, M.S., Zeng, S.X., Jin, Y., Sun, X.X., David, L., and Lu, H. (2004). Ribosomal protein L23 activates p53 by inhibiting MDM2 function in response to ribosomal perturbation but not to translation inhibition. Mol Cell Biol *24*, 7654-7668. 10.1128/mcb.24.17.7654-7668.2004.

6. Ofir-Rosenfeld, Y., Boggs, K., Michael, D., Kastan, M.B., and Oren, M. (2008). Mdm2 regulates p53 mRNA translation through inhibitory interactions with ribosomal protein L26. Mol Cell *32*, 180-189. 10.1016/j.molcel.2008.08.031.

7. Llanos, S., and Serrano, M. (2010). Depletion of ribosomal protein L37 occurs in response to DNA damage and activates p53 through the L11/MDM2 pathway. Cell Cycle *9*, 4005-4012. 10.4161/cc.9.19.13299.

8. Daftuar, L., Zhu, Y., Jacq, X., and Prives, C. (2013). Ribosomal proteins RPL37, RPS15 and RPS20 regulate the Mdm2-p53-MdmX network. PLoS One *8*, e68667. 10.1371/journal.pone.0068667.

9. He, X., Li, Y., Dai, M.S., and Sun, X.X. (2016). Ribosomal protein L4 is a novel regulator of the MDM2-p53 loop. Oncotarget *7*, 16217-16226. 10.18632/oncotarget.7479.

10. Dai, M.S., and Lu, H. (2004). Inhibition of MDM2-mediated p53 ubiquitination and degradation by ribosomal protein L5. J Biol Chem *279*, 44475-44482. 10.1074/jbc.M403722200.

11. Bai, D., Zhang, J., Xiao, W., and Zheng, X. (2014). Regulation of the HDM2-p53 pathway by ribosomal protein L6 in response to ribosomal stress. Nucleic Acids Res *42*, 1799-1811. 10.1093/nar/gkt971.

12. Zhou, X., Hao, Q., Liao, J., Zhang, Q., and Lu, H. (2013). Ribosomal protein S14 unties the MDM2-p53 loop upon ribosomal stress. Oncogene *32*, 388-396. 10.1038/onc.2012.63.

13. Chen, J., Wei, Y., Feng, Q., Ren, L., He, G., Chang, W., Zhu, D., Yi, T., Lin, Q., Tang, W., et al. (2016). Ribosomal protein S15A promotes malignant transformation and predicts poor outcome in colorectal cancer through misregulation of p53 signaling pathway. Int J Oncol *48*, 1628-1638. 10.3892/ijo.2016.3366.

14. Cho, J., Park, J., Shin, S.C., Kim, J.H., Kim, E.E., and Song, E.J. (2020). Ribosomal protein S2 interplays with MDM2 to induce p53. Biochem Biophys Res Commun *523*, 542-547. 10.1016/j.bbrc.2020.01.038.

15. Zhang, X., Wang, W., Wang, H., Wang, M.H., Xu, W., and Zhang, R. (2013). Identification of ribosomal protein S25 (RPS25)-MDM2-p53 regulatory feedback loop. Oncogene *32*, 2782-2791. 10.1038/onc.2012.289.

16. Cui, D., Li, L., Lou, H., Sun, H., Ngai, S.M., Shao, G., and Tang, J. (2014). The ribosomal protein S26 regulates p53 activity in response to DNA damage. Oncogene *33*, 2225-2235. 10.1038/onc.2013.170.

17. Xiong, X., Zhao, Y., He, H., and Sun, Y. (2011). Ribosomal protein S27-like and S27 interplay with p53-MDM2 axis as a target, a substrate and a regulator. Oncogene *30*, 1798-1811. 10.1038/onc.2010.569.

18. Sun, X.X., DeVine, T., Challagundla, K.B., and Dai, M.S. (2011). Interplay between ribosomal protein S27a and MDM2 protein in p53 activation in response to ribosomal stress. J Biol Chem *286*, 22730-22741. 10.1074/jbc.M111.223651.

19. Yadavilli, S., Mayo, L.D., Higgins, M., Lain, S., Hegde, V., and Deutsch, W.A. (2009). Ribosomal protein S3: A multi-functional protein that interacts with both p53 and MDM2 through its KH domain. DNA Repair (Amst) *8*, 1215-1224. 10.1016/j.dnarep.2009.07.003.